




Competing magnetic orders in quantum critical $\text{Sr}_3\text{Ru}_2\text{O}_7$

Aditya Putatunda ^{1,*}, Guanhua Qin,^{1,2,3,*} Wei Ren ^{2,3,†} and David J. Singh ^{1,4,‡}

¹*Department of Physics and Astronomy, University of Missouri, Columbia, Missouri 65211, USA*

²*Department of Physics, Shanghai University, Shanghai 200444, China*

³*Shanghai Key Laboratory of High Temperature Superconductors, MGI and ICQMS, Shanghai University, Shanghai 200444, China*

⁴*Department of Chemistry, University of Missouri, Columbia, Missouri 65211, USA*



(Received 19 March 2020; revised 29 May 2020; accepted 13 July 2020; published 23 July 2020)

We investigated $\text{Sr}_3\text{Ru}_2\text{O}_7$, a quantum critical metal that shows a metamagnetic quantum phase transition and electronic nematicity, through density functional calculations. These predict a ferromagnetic ground state in contrast to the experimentally observed paramagnetism, raising the question of competing magnetic states and associated fluctuations that may suppress magnetic order. We did a search to identify such low-energy antiferromagnetically ordered metastable states. We find that the lowest-energy antiferromagnetic state has a striped order. This corresponds to the E -type order that has been shown to be induced by Mn alloying. We also note significant transport anisotropy in this E -type ordered state. These results are discussed in relation to experimental observations.

DOI: [10.1103/PhysRevB.102.014442](https://doi.org/10.1103/PhysRevB.102.014442)

I. INTRODUCTION

Quantum criticality, especially in the context of its material-dependent signatures, is of significant current interest [1,2]. Here, we investigate the competing orders present in the quantum critical metamagnet $\text{Sr}_3\text{Ru}_2\text{O}_7$ [3–6]. We find low-energy antiferromagnetically ordered states that energetically compete with ferromagnetism. Interestingly, the lowest-energy antiferromagnetic (AFM) states show substantial in-plane transport anisotropy, which we discuss in relation to nematicity.

Members of the Ruddlesden-Popper (RP) series of strontium ruthenate compounds, $\text{Sr}_{n+1}\text{Ru}_n\text{O}_{3n+1}$, have many interesting characteristics. The $n = \infty$ member SrRuO_3 is a rare $4d$ itinerant ferromagnet [7,8]. The $n = 1$ member Sr_2RuO_4 , however, is a known unconventional superconductor [9–11]. The $n = 2$ bilayer compound, $\text{Sr}_3\text{Ru}_2\text{O}_7$, the focus of the present work, shows quantum criticality under magnetic field. Its phase diagram shows a metamagnetic transition with a critical point that can be tuned to near zero temperature by applying magnetic field [3,12–15]. Borzi and co-workers reported a strong in-plane conductivity anisotropy in this near tetragonal compound around the critical point and characterized it as nematic [16,17]. More broadly, $\text{Sr}_3\text{Ru}_2\text{O}_7$ presents an interesting case of a nearly ferromagnetic (FM) $4d$ material with a layered crystal structure and considerable tunability of properties [18–28].

In general, various low-temperature properties of a system situated near a magnetic quantum critical point (QCP), including transport, are strongly influenced by its associated spin fluctuations, sometimes up to relatively high temperatures

[29–32]. This is the case in $\text{Sr}_3\text{Ru}_2\text{O}_7$, implying that the spin fluctuations associated with the critical point are relatively strong in this material. The underlying quantum fluctuations also lead to a suppression of magnetic order [33]. In addition, they also present challenges to the characterization of such systems [34]. Commonly employed density functional theory (DFT) approximations, such as the local density approximation (LDA), behave like a mean-field theory in this regard and do not capture the effect of such spin fluctuations that arise near a quantum critical point [35]. These large fluctuations lead to a systematic overestimation of ground state magnetizations in DFT calculations [36,37].

We note that the overestimation of magnetizations and magnetic moments in standard density functional calculations for materials is unusual. In weak and moderately correlated magnetic materials standard DFT yields generally good agreement with experiment. This includes materials such as the $3d$ ferromagnets (Fe, Co, Ni, and a wide variety of intermetallics based on them) [38–40], as well as the ferromagnetic perovskite SrRuO_3 [7,41], which is chemically and structurally very similar to $\text{Sr}_3\text{Ru}_2\text{O}_7$. In strongly correlated systems, such as Mott insulators, the moments are often strongly underestimated by standard DFT calculations. For example, in the undoped parents of the high-temperature cuprate superconductors, DFT calculations fail to produce the experimentally observed antiferromagnetic ground states [42]. In these systems, the Coulomb repulsion, which is needed to localize the electrons, is inadequately represented in standard DFT calculations. Adding an additional Hubbard U then improves the description, including reproduction of the ground state of undoped cuprates [43,44].

While such strongly correlated materials, where standard DFT calculations underestimate magnetic ordering and do not properly describe the ground state, are relatively common, materials where such calculations overestimate the magnetic moments are much less common. These are cases where spin

*These authors contributed equally to this work.

†renwei@shu.edu.cn

‡singhdj@missouri.edu

fluctuations, often associated with nearby quantum critical points, are strong enough to significantly reduce the bare DFT moments. This has been discussed in terms of a bare DFT energy surface as a function of magnetization that is then renormalized by spin fluctuations using a fluctuation amplitude and a fluctuation renormalized Landau theory analogous to lowest order self-consistent phonon theory [45–47]. Applying this in a quantitative way to predict the renormalized magnetic properties from first principles is not straightforward due to the difficulty in determining a cutoff to distinguish spin fluctuations associated with the critical point, not included in standard DFT, from higher-energy spin fluctuations that are included [36]. However, by comparing standard DFT calculations with experiment, estimates have been made of fluctuation amplitudes [36,37]. Not surprisingly, the addition of Coulomb correlations by methods such as LDA + U degrades agreement with experiment in these cases since it introduces shifts opposite to those needed [48]. Furthermore, the magnitude of this type of deviation between DFT and experiment has been used as a signature to identify materials near magnetic quantum critical points [37,49–51], including successful predictions confirmed by subsequent experiments, as in the cases of hydrated Na_xCoO_2 and YFe_2Ge_2 [52–58].

It is also of interest to note the connection of $\text{Sr}_3\text{Ru}_2\text{O}_7$ and its magnetism to other members of the RP series, $(\text{Sr}, \text{Ca})_{n+1}\text{Ru}_n\text{O}_{3n+1}$. As mentioned, SrRuO_3 is a ferromagnet [59] with itinerant character that is well described by LDA calculations as far as its magnetism is concerned [7,60–62]. Furthermore, details of its electronic structure, including, for example, LDA-based predictions of a negative spin polarization, have been confirmed in detail by experiments [63–65].

Theoretical work indicates significant sensitivity of the magnetism to structure in this compound [60,66,67]. Experimentally, alloying with Ca leads to increased distortion of the ideal perovskite structure through octahedral tilts. This is accompanied by a decrease in the magnetic ordering temperature until a critical point is reached at $\sim 70\%$ Ca, beyond which a highly renormalized near ferromagnetic metal is found [68,69].

The importance of octahedral tilts and rotation in relation to magnetism is also found in single-layer $(\text{Sr}, \text{Ca})_2\text{RuO}_4$. Sr_2RuO_4 is a paramagnetic Fermi liquid that exhibits unconventional superconductivity at low temperature [9–11]. There has been debate about the extent and nature of correlations in this material [70–73]. However, it is generally agreed that the Fermi surface agrees with that predicted by LDA calculations [74,75], although with mass renormalization [76,77], that spin fluctuations likely play an important role in the superconductivity [41,78,79] and that these spin fluctuations have a substantial itinerant origin. This itinerant behavior includes the observation of incommensurate spin fluctuations predicted on the basis of Fermi-surface nesting [80]. Alloying with Ca in $(\text{Sr}, \text{Ca})_2\text{RuO}_4$ again demonstrates sensitivity to structure. Initially there is an increasing ferromagnetic susceptibility as the octahedra rotate, followed by a crossover, and eventually near pure Ca_2RuO_4 the development of an antiferromagnetic insulating phase with a strong change in the Ru-O bond length reflecting distortion of the octahedra [81,82].

In any case, the fluctuation-dissipation theorem, which relates the amplitude of the fluctuations to the dissipation,

given by an integral involving the imaginary part of the susceptibility, implies an enhanced imaginary component of the magnetic susceptibility associated with the sizable fluctuations in materials near magnetic quantum critical points. This in turn points towards the presence of strongly competing orders in materials that show strong spin fluctuations but no order, as discussed previously [46]. Besides an overly strong tendency towards ferromagnetism, both FM and AFM fluctuations [29,83] may coexist in this ruthenate system [30,79]. Here we report a search for such competing orders including commonly discussed AFM states as well as the so-called E -type order that occurs with heavy Mn doping [84].

II. COMPUTATIONAL METHODS

We searched initially for various possible magnetic orders using projector augmented wave (PAW) pseudopotentials as implemented in the Vienna *Ab initio* Simulation Package (VASP) [85,86]. An energy cutoff of 500 eV was used. Energy and force convergence criteria were chosen as 10^{-7} eV and 0.01 eV \AA^{-1} , respectively. The Brillouin zone (BZ), in this case, was sampled on a $5 \times 5 \times 5$ \mathbf{k} mesh. We used both LDA and the Perdew-Burke-Ernzerhof (PBE) generalized gradient approximation [87]. We also checked the structural predictions of these two functionals. We find that the PBE functional leads to a unit cell volume 1.6% larger than experiment (average lattice parameter error of +0.5%), while the LDA leads to an underestimate of the unit cell volume by 6.6% (average lattice parameter error of -2.2%). These are within the range of typical errors for these functionals and the somewhat smaller lattice parameters predicted by LDA relative to PBE is also as usual.

Following this survey, we then investigated the low-lying states in detail using the general potential linearized augmented plane wave (LAPW) [88] method as implemented in the WIEN2K code [89]. The LAPW sphere radii for Ru and Sr atoms were both chosen as $R_{MT} = 2.1$ bohrs, while for O atoms $R_{MT} = 1.55$ bohrs was used. The basis size was set by plane-wave cutoff K_{\max} with $R_{\min}K_{\max} = 7.0$. This leads to an effective $RK_{\max} = 9.5$ for the metal atoms. The self-consistent calculations were performed using a BZ sampling of at least 1000 \mathbf{k} points in the respective BZs. Transport integrals were done using the BOLTZTRAP code [90]. Dense Brillouin zone sampling with \mathbf{k} meshes of dimensions $30 \times 16 \times 16$ or higher was used for these calculations.

$\text{Sr}_3\text{Ru}_2\text{O}_7$ has a layered perovskite structure that is formed by two sheets of corner-sharing RuO_6 octahedra connected via a shared apical oxygen (Fig. 1). Interestingly, the metal ions still occupy the ideal tetragonal symmetry sites similar to the $n = 1$ compound Sr_2RuO_4 , although the Ru-O-Ru bonds are bent due to the counter-rotation of the octahedra about the c axis. These rotations amount to approximately 7° and are opposite for the two sheets making up a bilayer. This in combination with the stacking of the bilayers reduces the overall symmetry so that finally the compound has an orthorhombic crystal structure, space group $Ccca$ (No. 68) [31,91–93].

The lattice parameters for our calculations were taken from experiment, specifically the measurements performed on single crystals, as reported by Kiyonagi *et al.* [18]. These

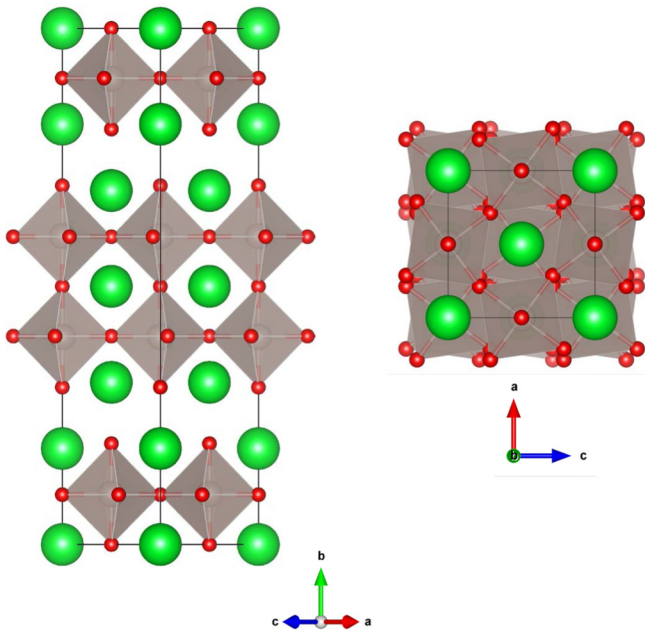


FIG. 1. Crystal structure of orthorhombic $\text{Sr}_3\text{Ru}_2\text{O}_7$, showing layering along c (left) and the view along the c axis, illustrating octahedral rotations (right).

are $a = 5.4979 \text{ \AA}$, $b = 5.5008 \text{ \AA}$, and $c = 26.7327 \text{ \AA}$. The internal positions of the atoms were relaxed. Details of the structure are in the Supplemental Material [94].

III. RESULTS AND DISCUSSION

A. Magnetic order

$\text{Sr}_3\text{Ru}_2\text{O}_7$ is a known metal and despite having a susceptibility peak at around $\sim 18 \text{ K}$ [22,92], it displays no long-range magnetic order [21]. Multiple reports, however, suggest temperature-dependent competing FM and AFM spin fluctuations, although the nature of the AFM fluctuations has not been established [26,29,95–99].

Both experimental and theoretical investigations show that the material lies close to a magnetic instability [21,23,100]. Apart from applying an external magnetic field along various directions, investigations by perturbing the system via uniaxial pressure [91,101,102], doping by both magnetic impurities [23,24] and nonmagnetic impurities [96,103] find various magnetic behaviors. DFT investigations find a ferromagnetic instability in contrast to the experimentally observed enhanced paramagnetic state [21,104,105]. As mentioned, this type of error is a characteristic of a material near a quantum critical point. In the case of $\text{Sr}_3\text{Ru}_2\text{O}_7$, the predicted ferromagnetism has an itinerant origin, coming from a high density of states associated with the structure of the t_{2g} bands, specifically Van Hove singularities in the d_{xy} band. This Stoner mechanism is similar to SrRuO_3 and Sr_2RuO_4 [25,41,60,104,106]. The finding of an incorrect ferromagnetic state is not affected by spin-orbit coupling. In our calculations, which were done in a scalar relativistic approximation, we found a spin magnetization of $4.7\mu_B$ per unit cell (four Ru atoms, including the interstitial and O components) in the LDA, which is reduced by less than 10% to $4.4\mu_B$ per cell

when spin orbit is included. Adding Coulomb correlations using the LDA + U method [44], with a moderate value $U = 4 \text{ eV}$ and the standard fully localized limit double counting strongly increases the magnetization to $7.9\mu_B$ per cell, opposite to what is needed to produce agreement with experiment. This is not unexpected, since degradation of standard DFT results with the addition of U has been noted in other itinerant magnetic systems previously [40,107].

As mentioned, $\text{Sr}_3\text{Ru}_2\text{O}_7$ displays a metamagnetic transition at a field strength of approximately 7–8 T [4]. However, doping using magnetic impurities [108] such as Fe [23] and Mn [24,27,84,109,110] as well as nonmagnetic Ti [103] has been found to yield different AFM orders [108]. In general, the relationship between these and the properties of the undoped compound is unclear, since these dopants produce strong perturbations of the system. Nonetheless, one notable order is the double stripe E -type order that is observed with heavy Mn doping [84], although it is reported to have a short correlation length [23,84]. It is to be noted that in particular it is quite unclear that the E -type order found in Mn-doped samples is reflective of the properties of undoped $\text{Sr}_3\text{Ru}_2\text{O}_7$. This is because the Mn doping is also accompanied by sizable distortions in the crystal structure along with bandwidth changes that may stabilize antiferromagnetic structures [111,112]. Furthermore, doping in $\text{Sr}_3\text{Ru}_2\text{O}_7$ is often accompanied with transition to a state of more insulating transport [23,24,84,103,111,113], while pristine $\text{Sr}_3\text{Ru}_2\text{O}_7$ is clearly metallic and itinerant. This has led to a focus on other orders as possible competing orders to ferromagnetism in pristine $\text{Sr}_3\text{Ru}_2\text{O}_7$. For example, based on their hybrid functional calculations, Rivero and co-workers reported other AFM orders both of metallic and insulating nature that may be obtained via strain, particularly a layered A -type AFM [101,114–116].

Here we performed a search for possible long-range AFM orders (within collinear magnetism) in relation to both FM and nonmagnetic orders initially through PAW calculations (Fig. 2). We find the FM state as the ground state for both LDA and PBE functionals. Besides the FM order, the lowest energies are for the E -type order. There are two such states that are slightly nondegenerate due to orthorhombicity. PBE shows stronger magnetism over LDA including larger magnetic energies and higher moments. The three other commonly discussed AFM states lie much higher in energy in the order, $A < C < G$ (Fig. 2). No self-consistent solution was found for the G -type order within the LDA. The bottom six S -labeled AFM orders lie somewhere in the middle of the whole range. Details of the magnetic energies as obtained from these initial PAW calculations are in the Supplemental Material (SM) [94].

The lack of solution for G type and the variability of the moments between the different states is a characteristic of itinerant magnetism, as is the fact that the energy differences between different orders are of similar order to the energy difference between the non-spin-polarized and the lowest-energy FM state. Thus local moment pictures, such as short-range Heisenberg models, are not well suited to this material. Furthermore, the A -type order, which consists of oppositely aligned FM layers stacked across the bilayer, lies much higher in energy than both of the E types and the FM order. This

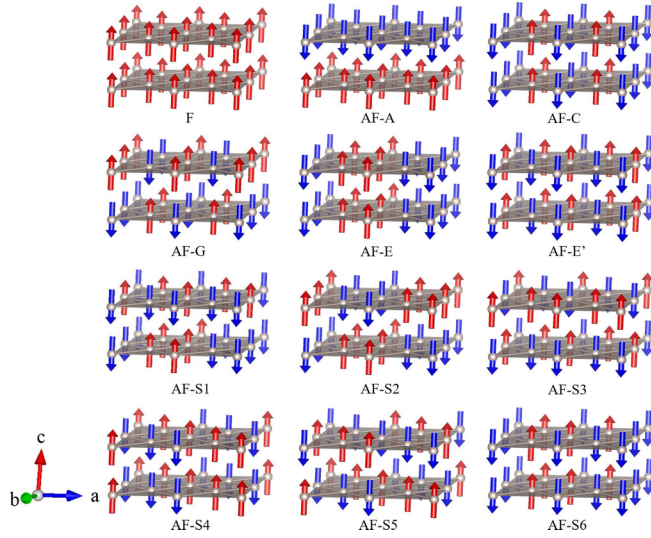


FIG. 2. Various magnetic configurations investigated. Only Ru atoms are shown. These include ferromagnetism, *A*-type, *G*-type, and *C*-type antiferromagnetism, which are common orders for perovskites, two *E*-type orders, which are slightly nondegenerate due to the orthorhombic crystal symmetry, and more complex orders with larger unit cells.

means that interactions between the layers within a bilayer are strong.

We now turn to the detailed results obtained with the LAPW method [26,88]. The energetics and magnetic moments are in Table I. Most importantly, we find that the two metastable *E*-type AFM states carry large magnetic moments ($\sim 1.08\mu_B$ within PBE and $\sim 0.85\mu_B$ within LDA). As expected, these are the orders that consistently lie closest to the FM ground state.

The sizable moments obtained and the FM ground state contradict the fact that $\text{Sr}_3\text{Ru}_2\text{O}_7$ is an experimentally determined paramagnet. However, this is almost certainly due to

TABLE I. Energy ordering of various magnetic orders (per formula unit) found by LAPW calculations and their (absolute) averaged magnetic moments for both PBE and LDA functionals. Refer to Fig. 2 for naming. FM and nonmagnetic (NM) respectively stand for ferromagnetic and nonmagnetic state (zero-energy level), while all the other orders are antiferromagnetic in nature. Note that the moments reported here are those lying within the LAPW sphere radii.

Order	PBE		LDA	
	ΔE meV/f.u.	Magn. mom. Ru (μ_B)	ΔE meV/f.u.	Magn. mom. Ru (μ_B)
FM	-147.8	1.28	-29.9	0.73
<i>E</i>	-131.5	1.08	-28.6	0.85
<i>E'</i>	-130.3	1.08	-28.0	0.85
<i>A</i>	-95.6	1.06	-21.2	0.60
<i>C</i>	-43.6	0.72	-13.6	0.38
<i>G</i>	-3.2	0.45		
NM	0	0.000	0	0.000

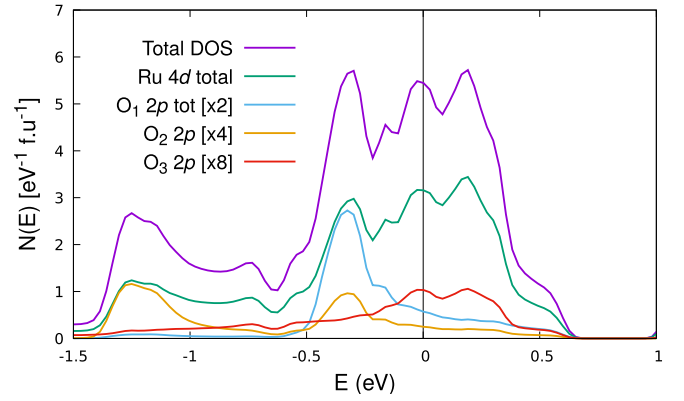


FIG. 3. Density of states per formula unit of $\text{Sr}_3\text{Ru}_2\text{O}_7$ for its nonmagnetic state showing the respective LAPW sphere projected contributions from Ru *4d* and O *2p* orbitals obtained within LDA. Three kinds of O contributions (scaled four times for visibility) are observed (see text) with their respective multiplicities, shown in parentheses. The black vertical line at $E = 0$ shows the Fermi level.

the fact that the system lies close to a magnetic QCP where strong spin fluctuations suppress any long-range magnetic order in the system. Standard DFT calculations fail to describe this type of fluctuations, as has been noted for other such materials near a magnetic QCP [26,37,117–119]. As mentioned, this overestimation of magnetism has been used as a signature of materials that are in the vicinity of a QCP [36,37,46,119].

In addition, one may note that the magnetic moments predicted for the *E*-type orders are indeed the largest among the AFM states. All the other investigated orders lie higher in energy and have lower magnetic moments. The energy difference within LDA between the FM and *E* orders is only 1.6 meV per formula unit on average (for the *E* and *E'*). Thus we find that the *E*-type order is very likely the order that competes with ferromagnetism in this material. It is interesting to note that the *E*-type order is also the order among the ones considered that breaks the tetragonal symmetry within the RuO_2 plane.

B. Electronic structure and transport

Our calculated electronic density of states (DOS) of nonmagnetic $\text{Sr}_3\text{Ru}_2\text{O}_7$, as shown in Fig. 3 shows a peak around the Fermi level. This favors magnetism through the Stoner mechanism as discussed previously [60]. For the considered *E*-type orders, the corresponding DOS (shown in the Supplemental Material) [94] is distorted but still high near the Fermi level. Table II summarizes the DOS value observed at the Fermi level, $N(E_F)$ for each investigated magnetic order. Table II shows that the electronic structure remains metallic for all the spin orderings considered. As noted previously, there is strong Ru *4d*-O *2p* hybridization evident.

The individual contributions from each of the three different types of O atoms are labeled. It can be noted that the *2p* contribution from the O3 atoms, which are the in-plane O, is the largest in the region closest around the Fermi level. It reaffirms the fact that the material is highly two dimensional and most of the electronic transport occurs primarily in-plane.

TABLE II. Density of states (per formula unit) at the Fermi level, $N(E_F)$ of $\text{Sr}_3\text{Ru}_2\text{O}_7$ for various magnetic orders with both LDA and PBE functionals. Note that for the ferromagnetic order (FM), and for other magnetic orders, $N(E_F)$ for each single spin channel (\uparrow, \downarrow) is shown. A Gaussian broadening of 4 meV was used. Units are $1/\text{eV}$.

Order	LAPW			
	LDA		PBE	
FM (\uparrow, \downarrow)	3.9	3.4	0.9	4.8
E	5.0		4.5	
E'	5.4		4.7	
A	4.0		3.0	
C	7.8		7.1	
NM	5.4		6.4	

O1 and O2 are respectively the shared and SrO layer apical oxygen atoms and contribute less near the Fermi level.

In an octahedral crystal field, the d orbitals split into a lower-lying t_{2g} manifold, with three bands (and six electrons) and a higher-lying e_g manifold that can accommodate four electrons. The e_g manifold is derived from σ antibonding combinations of O p and Ru d orbitals, while the normally more narrow t_{2g} manifold consists of more weakly antibonding π combinations. Ru^{4+} , as in $\text{Sr}_3\text{Ru}_2\text{O}_7$, has four d electrons, which leads to a partially filled t_{2g} manifold that is responsible for the magnetism and transport. The electronic DOS in the region near the Fermi level is derived from hybridized Ru t_{2g} and O p states.

The orbital character is often important in understanding magnetic ordering, especially in systems where transition metal–O hybridization is important, for example double exchange systems [120]. Figure 4 shows the projections of Ru d onto a site with the different magnetic orders as obtained with

the PBE functional. As noted previously, non-spin-polarized $\text{Sr}_3\text{Ru}_2\text{O}_7$ has a relatively narrow set of nominally t_{2g} orbitals [104]. It should be noted, however, that this crystal-field notation is not strictly correct since the octahedral rotation mixes the e_g and t_{2g} manifolds, and the layered structure splits the t_{2g} orbitals. There is also mixing due to symmetry lowering associated with magnetic order as well as splitting due to interactions between the two layers forming a bilayer.

However, we find that the general shape of the DOS in the energy range of the t_{2g} orbitals does not depend strongly on magnetic order, showing a higher peak around the Fermi level against a broader peak at ~ -1 eV. The main effect of magnetism is to exchange split this peak into a lower-lying majority and higher-lying minority components, with the largest exchange splitting for the orders where the moment is highest. The second aspect to note is that the E -type order gives a strong narrowing of the individual DOS peaks in the t_{2g} manifold. This leads to a greater differentiation of the orbitals. This is also the case for the C -type and G -type orders, which have nearest-neighbor antiferromagnetism in a single plane. Meanwhile the lowest-energy ferromagnetic and the A -type order have generally broader individual peaks.

In Tables III and IV, we show the reduced electrical conductivity (σ/τ) values for different orders obtained using both LDA and PBE functionals. The transport integrals were done for a temperature of 100 K in the Fermi function for computational convenience. These were calculated using the BOLTZTRAP code [90]. The BOLTZTRAP code constructs a smooth interpolation of the energy bands that passes through all the first-principles points. In our calculations we used dense first-principles meshes consisting of $30 \times 16 \times 16$ grids or better so that the interpolated bands are accurate. The BOLTZTRAP code then does transport integrals using this interpolation to construct the gradients that comprise the band velocities.

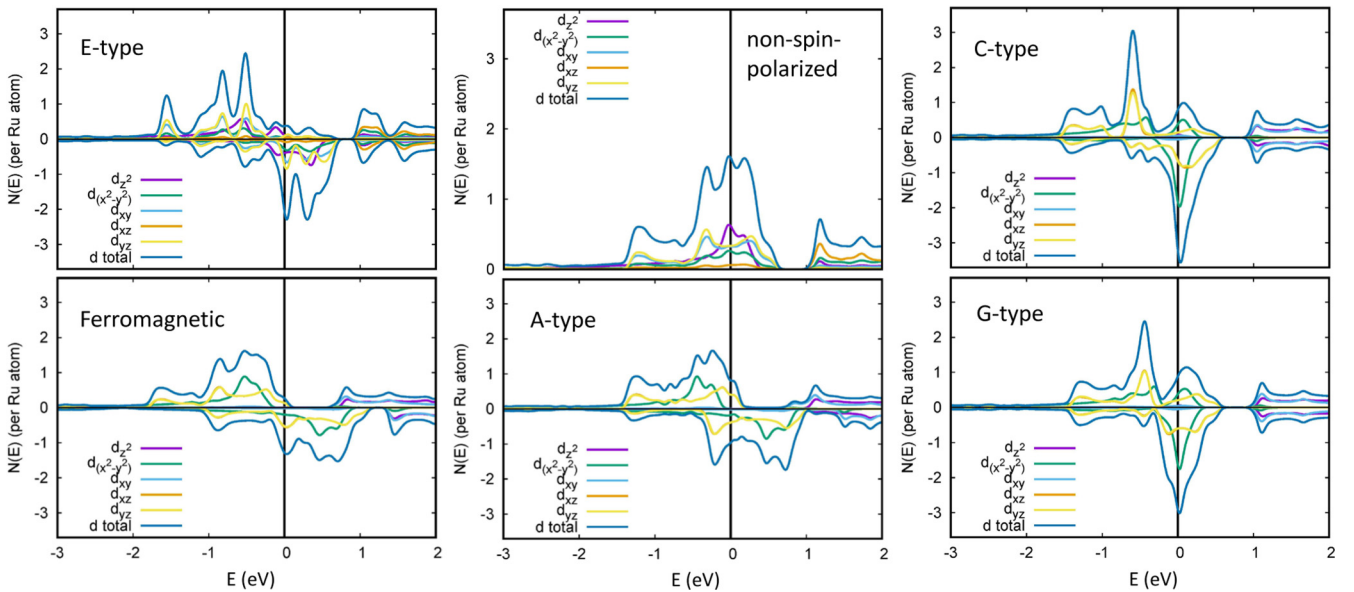


FIG. 4. Projected DOS of d character on a Ru atom in the energy range of the t_{2g} bands for the different magnetic orderings as obtained with the PBE functional. Note that the individual d orbitals are mixed because of the low symmetry induced by the octahedral rotations and magnetic order. The same symmetry was used for the E -type and non-spin-polarized. The ferromagnetic, A -type, C -type, and G -type were done in a smaller higher-symmetry cell which leads to a different coordinate system for the d orbitals.

TABLE III. In-plane components of the diagonalized reduced electrical conductivity tensor and the corresponding anisotropies for various magnetic orders with the LDA functional.

Order	σ/τ [$10^{18} (\Omega \text{ ms})^{-1}$]		In-plane anisotropy
E	65	77	1.17
E'	67	75	1.13
A	249	250	1.00
FM (\uparrow)	159	161	1.01
(\downarrow)	191	191	1.00
C	229	233	1.02
NM	266	274	1.03

To ensure consistency across various magnetic orders, the conductivity tensors have been appropriately diagonalized and only the in-plane directions are given. These are the two largest eigenvalues of the conductivity tensor. In Tables III and IV, the out-of-plane reduced conductivity components, being about two orders smaller than the in-plane components have been omitted.

As seen in Tables III and IV, noticeable anisotropy occurs among the in-plane conductivity components only in the case of the E -type magnetic order. These anisotropy values are noticeably larger than those obtained for any other orders. One may note that within LDA, the in-plane (reduced) electrical conductivity values differ by about $\sim 15\%$. While it is perhaps not surprising that the E -type order gives more anisotropy considering that the pattern of magnetic moments in the RuO_2 planes is anisotropic with this order, unlike other simple orders, it is important that this anisotropy in the magnetic pattern is indeed well reflected in the electronic structure at the Fermi level that controls transport. The higher-symmetry (and lower-energy) E -type order is slightly more anisotropic than the E' order. In PBE, however, the anisotropies are larger. This reflects its tendency towards larger moments. In this case, when contrasted to LDA, the ordering is reversed and E' order has higher anisotropy.

It is interesting to note that in their investigation Borzi *et al.* [17] found an in-plane resistivity anisotropy value of $\sim 20\%$ near their lowest reported experimental temperature. This is within the range of the conductivity anisotropies found for the E -type orders, for example, $\sim 15\%$ on average for the LDA

TABLE IV. In-plane components of the diagonalized reduced electrical conductivity tensor and their corresponding anisotropies for various magnetic orders with the PBE functional.

Order	σ/τ [$10^{18} (\Omega \text{ ms})^{-1}$]		In-plane anisotropies
E	27	49	1.77
E'	24	47	1.95
A	174	177	1.01
FM (\uparrow)	11.4	11.5	1.01
(\downarrow)	218	222	1.02
C	187	189	1.01
G	248	256	1.03
NM	256	264	1.03

and the larger values for the PBE functional, which has larger moments.

IV. SUMMARY AND CONCLUSIONS

We investigated $\text{Sr}_3\text{Ru}_2\text{O}_7$, a quantum critical material to identify its low-lying antiferromagnetic metastable states that might contribute to the strong spin fluctuations that are thought to strongly affect its properties. We find that the energetically lowest metastable states carry a striped E -type AFM ordering. The corresponding transport properties show sizable in-plane conductivity anisotropy in contrast to other possible AFM orders. Experimental investigation using inelastic neutron scattering in search of spin fluctuations arising from this E -type order will be of interest.

ACKNOWLEDGMENTS

Work at the University of Missouri is supported by the Department of Energy, Basic Energy Sciences award DE-SC0019114. G.Q. is grateful for support from the China Scholarship Council (CSC). Support for work at Shanghai University is provided by the National Natural Science Foundation of China (Grants No. 51672171, No. 51861145315, and No. 51911530124), Independent Research Project of State Key Laboratory of Advanced Special Steel and Shanghai Key Laboratory of Advanced Ferrometallurgy at Shanghai University, and the fund of the State Key Laboratory of Solidification Processing in NWPU (Grant No. SKLSP201703).

[1] S. Sachdev, *Quantum Phase Transitions*, 2nd ed. (Cambridge University Press, Cambridge, UK, 2011).
[2] P. Gegenwart, Q. Si, and F. Steglich, *Nat. Phys.* **4**, 186 (2008).
[3] S. A. Grigera, R. S. Perry, A. J. Schofield, M. Chiao, S. R. Julian, G. G. Lonzarich, S. I. Ikeda, Y. Maeno, A. J. Millis, and A. P. Mackenzie, *Science* **294**, 329 (2001).
[4] Y. Tokiwa, M. Mchawat, R. S. Perry, and P. Gegenwart, *Phys. Rev. Lett.* **116**, 226402 (2016).
[5] K. Iwaya, S. Satow, T. Hanaguri, N. Shannon, Y. Yoshida, S. I. Ikeda, J. P. He, Y. Kaneko, Y. Tokura, T. Yamada, and H. Takagi, *Phys. Rev. Lett.* **99**, 057208 (2007).

[6] W. Wu, A. McCollam, S. A. Grigera, R. S. Perry, A. P. Mackenzie, and S. R. Julian, *Phys. Rev. B* **83**, 045106 (2011).
[7] D. J. Singh, *J. Appl. Phys.* **79**, 4818 (1996).
[8] P. B. Allen, H. Berger, O. Chauvet, L. Forro, T. Jarlborg, A. Junod, B. Revaz, and G. Santi, *Phys. Rev. B* **53**, 4393 (1996).
[9] Y. Maeno, H. Hashimoto, K. Yoshida, S. Nishizaki, T. Fujita, J. G. Bednorz, and F. Lichtenberg, *Nature (London)* **372**, 532 (1994).
[10] K. Ishida, H. Mukuda, Y. Kitaoka, K. Asayama, Z. Q. Mao, Y. Mori, and Y. Maeno, *Nature (London)* **396**, 658 (1998).
[11] A. Pustogow, Y. Luo, A. Chronister, Y.-S. Su, D. A. Sokolov, F. Jerzembeck, A. P. Mackenzie, C. W. Hicks, N. Kikugawa,

- S. Raghu, E. D. Bauer, and S. E. Brown, *Nature (London)* **574**, 72 (2019).
- [12] C. Lester, S. Ramos, R. S. Perry, T. P. Croft, R. I. Bewley, T. Guidi, P. Manuel, D. D. Khalyavin, E. M. Forgan, and S. M. Hayden, *Nat. Mater.* **14**, 373 (2015).
- [13] S. A. Grigera, R. A. Borzi, A. P. Mackenzie, S. R. Julian, R. S. Perry, and Y. Maeno, *Phys. Rev. B* **67**, 214427 (2003).
- [14] J. A. N. Bruin, R. A. Borzi, S. A. Grigera, A. W. Rost, R. S. Perry, and A. P. Mackenzie, *Phys. Rev. B* **87**, 161106(R) (2013).
- [15] C. M. Puetter, J. G. Rau, and H.-Y. Kee, *Phys. Rev. B* **81**, 081105(R) (2010).
- [16] E. Fradkin, S. A. Kivelson, M. J. Lawler, J. P. Eisenstein, and A. P. Mackenzie, *Annu. Rev. Condens. Matter Phys.* **1**, 153 (2010).
- [17] R. A. Borzi, S. A. Grigera, J. Farrell, R. S. Perry, S. J. S. Lister, S. L. Lee, D. A. Tennant, Y. Maeno, and A. P. Mackenzie, *Science* **315**, 214 (2007).
- [18] R. Kiyonagi, K. Tsuda, N. Aso, H. Kimura, Y. Noda, Y. Yoshida, S.-I. Ikeda, and Y. Uwatoko, *J. Phys. Soc. Jpn.* **73**, 639 (2004).
- [19] R. Cava, H. Zandbergen, J. Krajewski, W. Peck, B. Batlogg, S. Carter, R. Fleming, O. Zhou, and L. Rupp, *J. Solid State Chem.* **116**, 141 (1995).
- [20] G. Cao, S. McCall, and J. E. Crow, *Phys. Rev. B* **55**, R672(R) (1997).
- [21] S.-I. Ikeda, Y. Maeno, S. Nakatsuji, M. Kosaka, and Y. Uwatoko, *Phys. Rev. B* **62**, R6089(R) (2000).
- [22] S.-I. Ikeda and Y. Maeno, *Phys. B: Condens. Matter* **259-261**, 947 (1999).
- [23] M. Zhu, Y. Wang, P. G. Li, J. J. Ge, W. Tian, D. Keavney, Z. Q. Mao, and X. Ke, *Phys. Rev. B* **95**, 174430 (2017).
- [24] R. Mathieu, A. Asamitsu, Y. Kaneko, J. P. He, X. Z. Yu, R. Kumai, Y. Onose, N. Takeshita, T. Arima, H. Takagi, and Y. Tokura, *Phys. Rev. B* **72**, 092404 (2005).
- [25] A. Tamai, M. P. Allan, J. F. Mercure, W. Meevasana, R. Dunkel, D. H. Lu, R. S. Perry, A. P. Mackenzie, D. J. Singh, Z.-X. Shen, and F. Baumberger, *Phys. Rev. Lett.* **101**, 026407 (2008).
- [26] I. I. Mazin, M. D. Johannes, L. Boeri, K. Koepernik, and D. J. Singh, *Phys. Rev. B* **78**, 085104 (2008).
- [27] C. Chen, J. Kim, V. B. Nascimento, Z. Diao, J. Teng, B. Hu, G. Li, F. Liu, J. Zhang, R. Jin, and E. W. Plummer, *Phys. Rev. B* **94**, 085420 (2016).
- [28] M. P. Allan, A. Tamai, E. Rozbicki, M. H. Fischer, J. Voss, P. D. C. King, W. Meevasana, S. Thirupathiah, E. Rienks, J. Fink, D. A. Tennant, R. S. Perry, J. F. Mercure, M. A. Wang, J. Lee, C. J. Fennie, E. A. Kim, M. J. Lawler, K. M. Shen, A. P. Mackenzie, Z. X. Shen, and F. Baumberger, *New J. Phys.* **15**, 063029 (2013).
- [29] L. Capogna, E. M. Forgan, S. M. Hayden, A. Wildes, J. A. Duffy, A. P. Mackenzie, R. S. Perry, S. Ikeda, Y. Maeno, and S. P. Brown, *Phys. Rev. B* **67**, 012504 (2003).
- [30] K. Kitagawa, K. Ishida, R. S. Perry, T. Tayama, T. Sakakibara, and Y. Maeno, *Phys. Rev. Lett.* **95**, 127001 (2005).
- [31] H. Shaked, J. Jorgensen, O. Chmaissem, S. Ikeda, and Y. Maeno, *J. Solid State Chem.* **154**, 361 (2000).
- [32] M. B. Stone, M. D. Lumsden, R. Jin, B. C. Sales, D. Mandrus, S. E. Nagler, and Y. Qiu, *Phys. Rev. B* **73**, 174426 (2006).
- [33] T. Moriya, *Spin Fluctuations in Itinerant Electron Magnetism* (Springer, Berlin, 2012), Vol. 56.
- [34] R. B. Laughlin, G. G. Lonzarich, P. Monthoux, and D. Pines, *Adv. Phys.* **50**, 361 (2001).
- [35] A. Aguayo, I. I. Mazin, and D. J. Singh, *Phys. Rev. Lett.* **92**, 147201 (2004).
- [36] P. Larson, I. I. Mazin, and D. J. Singh, *Phys. Rev. B* **69**, 064429 (2004).
- [37] I. I. Mazin and D. J. Singh, *Phys. Rev. B* **69**, 020402(R) (2004).
- [38] O. Gunnarsson, *J. Phys. F: Met. Phys.* **6**, 587 (1976).
- [39] A. R. Williams, V. L. Moruzzi, C. D. Gelatt, Jr., J. Kubler, and K. Schwarz, *J. Appl. Phys.* **53**, 2019 (1982).
- [40] Y. Fu and D. J. Singh, *Phys. Rev. B* **100**, 045126 (2019).
- [41] I. I. Mazin and D. J. Singh, *Phys. Rev. Lett.* **79**, 733 (1997).
- [42] W. E. Pickett, *Rev. Mod. Phys.* **61**, 433 (1989).
- [43] V. I. Anisimov, F. Aryasetiawan, and A. I. Lichtenstein, *J. Phys.: Condens. Matter* **9**, 767 (1997).
- [44] S. L. Dudarev, G. A. Botton, S. Y. Savrasov, C. J. Humphreys, and A. P. Sutton, *Phys. Rev. B* **57**, 1505 (1998).
- [45] M. Shimizu, *Rep. Prog. Phys.* **44**, 329 (1981).
- [46] S. N. Kaul, *J. Phys.: Condens. Matter* **11**, 7597 (1999).
- [47] T. Moriya, *Spin Fluctuations in Itinerant Electron Magnetism* (Springer, Berlin, 1985).
- [48] M. D. Johannes, I. I. Mazin, and D. J. Singh, *Phys. Rev. B* **71**, 205103 (2005).
- [49] A. Leithe-Jasper, W. Schnelle, H. Rosner, M. Baenitz, A. Rabis, A. A. Gippius, E. N. Morozova, H. Borrmann, U. Burkhardt, R. Ramlau, U. Schwarz, J. A. Mydosh, Y. Grin, V. Ksenofontov, and S. Reiman, *Phys. Rev. B* **70**, 214418 (2004).
- [50] V. V. Krishnamurthy, J. C. Lang, D. Haskel, D. J. Keavney, G. Srajer, J. L. Robertson, B. C. Sales, D. G. Mandrus, D. J. Singh, and D. I. Bilc, *Phys. Rev. Lett.* **98**, 126403 (2007).
- [51] D. J. Singh, *Phys. Rev. B* **93**, 245155 (2016).
- [52] D. J. Singh, *Phys. Rev. B* **68**, 020503(R) (2003).
- [53] Y. Ihara, H. Takeya, K. Ishida, H. Ikeda, C. Michioka, K. Takada, T. Sasaki, H. Sakurai, and E. Takayama-Muromachi, *J. Phys. Soc. Jpn.* **75**, 124714 (2006).
- [54] Y. Ihara, H. Takeya, K. Ishida, C. Michioka, K. Yoshimura, K. Takada, T. Sasaki, H. Sakurai, and E. Takayama-Muromachi, *Phys. Rev. B* **75**, 212506 (2007).
- [55] D. J. Singh, *Phys. Rev. B* **89**, 024505 (2014).
- [56] N. Sirica, F. Bondino, S. Nappini, I. Pis, L. Poudel, A. D. Christianson, D. Mandrus, D. J. Singh, and N. Mannella, *Phys. Rev. B* **91**, 121102(R) (2015).
- [57] D. Zhao, H. L. Wo, J. Li, D. W. Song, L. X. Zheng, S. J. Li, L. P. Nie, X. G. Luo, J. Zhao, T. Wu, and X. H. Chen, *Phys. Rev. B* **101**, 064511 (2020).
- [58] H. Wo, Q. Wang, Y. Shen, X. Zhang, Y. Hao, Y. Feng, S. Shen, Z. He, B. Pan, W. Wang, K. Nakajima, S. Ohira-Kawamura, P. Steffens, M. Boehm, K. Schmalzl, T. R. Forrest, M. Matsuda, Y. Zhao, J. W. Lynn, Z. Yin, and J. Zhao, *Phys. Rev. Lett.* **122**, 217003 (2019).
- [59] A. Kanbayashi, *J. Phys. Soc. Jpn.* **44**, 108 (1978).
- [60] I. I. Mazin and D. J. Singh, *Phys. Rev. B* **56**, 2556 (1997).
- [61] K. Maiti and R. S. Singh, *Phys. Rev. B* **71**, 161102(R) (2005).
- [62] N. Miao, N. C. Bristowe, B. Xu, M. J. Verstraete, and P. Gosez, *J. Phys.: Condens. Matter* **26**, 035401 (2014).
- [63] B. Nadgorny, M. S. Osofsky, D. J. Singh, G. T. Woods, and R. J. Soulen, Jr., *Appl. Phys. Lett.* **82**, 427 (2003).

- [64] P. Raychaudhuri, A. P. Mackenzie, J. W. Reiner, and M. R. Beasley, *Phys. Rev. B* **67**, 020411(R) (2003).
- [65] D. C. Worledge and T. H. Geballe, *Phys. Rev. Lett.* **85**, 5182 (2000).
- [66] J. M. Rondinelli, N. M. Caffrey, S. Sanvito, and N. A. Spaldin, *Phys. Rev. B* **78**, 155107 (2008).
- [67] A. T. Zayak, X. Huang, J. B. Neaton, and K. M. Rabe, *Phys. Rev. B* **74**, 094104 (2006).
- [68] G. Cao, O. Korneta, S. Chikara, L. E. DeLong, and P. Schlottmann, *Solid State Commun.* **148**, 305 (2008).
- [69] N. Kikugawa, L. Balicas, and A. P. Mackenzie, *J. Phys. Soc. Jpn.* **78**, 014701 (2009).
- [70] Z. V. Pchelkina, I. A. Nekrasov, T. Pruschke, A. Sekiyama, S. Suga, V. I. Anisimov, and D. Vollhardt, *Phys. Rev. B* **75**, 035122 (2007).
- [71] D. J. Singh, *Phys. Rev. B* **77**, 046101 (2008).
- [72] N. J. C. Ingle, K. M. Shen, F. Baumberger, W. Meevasana, D. H. Lu, Z.-X. Shen, S. Nakatsuji, Z. Q. Mao, Y. Maeno, T. Kimura, and Y. Tokura, *Phys. Rev. B* **72**, 205114 (2005).
- [73] A. Damascelli, D. H. Lu, K. M. Shen, N. P. Armitage, F. Ronning, D. L. Feng, C. Kim, Z. X. Shen, T. Kimura, Y. Tokura, Z. Q. Mao, and Y. Maeno, *Phys. Rev. Lett.* **85**, 5194 (2000).
- [74] T. Oguchi, *Phys. Rev. B* **51**, 1385(R) (1995).
- [75] D. J. Singh, *Phys. Rev. B* **52**, 1358 (1995).
- [76] T. Katsufuji, M. Kasai, and Y. Tokura, *Phys. Rev. Lett.* **76**, 126 (1996).
- [77] C. Bergemann, S. R. Julian, A. P. Mackenzie, S. NishiZaki, and Y. Maeno, *Phys. Rev. Lett.* **84**, 2662 (2000).
- [78] M. Sigrist, D. Agterberg, T. M. Rice, and M. E. Zhitomirsky, *Physica C* **282-287**, 214 (1997).
- [79] I. I. Mazin and D. J. Singh, *Phys. Rev. Lett.* **82**, 4324 (1999).
- [80] M. Braden, Y. Sidis, P. Bourges, P. Pfeuty, J. Kulda, Z. Mao, and Y. Maeno, *Phys. Rev. B* **66**, 064522 (2002).
- [81] S. Nakatsuji, S. I. Ikeda, and Y. Maeno, *J. Phys. Soc. Jpn.* **66**, 1868 (1997).
- [82] J. P. Carlo, T. Goko, I. M. Gat-Malureanu, P. R. Russo, A. T. Savici, A. A. Aczel, G. J. MacDougall, J. A. Rodriguez, T. J. Williams, G. M. Luke, C. R. Wiebe, Y. Yoshida, S. Nakatsuji, Y. Maeno, T. Taniguchi, and Y. J. Uemura, *Nat. Mater.* **11**, 323 (2012).
- [83] R. Perry, L. Galvin, A. Mackenzie, D. Forsythe, S. Julian, S. Ikeda, and Y. Maeno, *Physica B: Condens. Matter* **284-288**, 1469 (2000).
- [84] D. Mesa, F. Ye, S. Chi, J. A. Fernandez-Baca, W. Tian, B. Hu, R. Jin, E. W. Plummer, and J. Zhang, *Phys. Rev. B* **85**, 180410(R) (2012).
- [85] G. Kresse and J. Furthmüller, *Phys. Rev. B* **54**, 11169 (1996).
- [86] G. Kresse and D. Joubert, *Phys. Rev. B* **59**, 1758 (1999).
- [87] J. P. Perdew, K. Burke, and M. Ernzerhof, *Phys. Rev. Lett.* **77**, 3865 (1996).
- [88] D. J. Singh and L. Nordstrom, *Planewaves, Pseudopotentials, and the LAPW Method*, 2nd ed. (Springer, Berlin, 2006).
- [89] K. Schwarz, P. Blaha, and G. K. H. Madsen, *Comput. Phys. Commun.* **147**, 71 (2002).
- [90] G. K. H. Madsen and D. J. Singh, *Comput. Phys. Commun.* **175**, 67 (2006).
- [91] S.-I. Ikeda, N. Shirakawa, T. Yanagisawa, Y. Yoshida, S. Koikegami, S. Koike, M. Kosaka, and Y. Uwatoko, *J. Phys. Soc. Jpn.* **73**, 1322 (2004).
- [92] Q. Huang, J. W. Lynn, R. W. Erwin, J. Jarupatrakorn, and R. J. Cava, *Phys. Rev. B* **58**, 8515 (1998).
- [93] B. Hu, G. T. McCandless, M. Menard, V. B. Nascimento, J. Y. Chan, E. W. Plummer, and R. Jin, *Phys. Rev. B* **81**, 184104 (2010).
- [94] See Supplemental Material at <http://link.aps.org/supplemental/10.1103/PhysRevB.102.014442> for information on pseudopotential results and details of the crystal structure.
- [95] R. S. Perry, L. M. Galvin, S. A. Grigera, L. Capogna, A. J. Schofield, A. P. Mackenzie, M. Chiao, S. R. Julian, S. I. Ikeda, S. Nakatsuji, Y. Maeno, and C. Pfleiderer, *Phys. Rev. Lett.* **86**, 2661 (2001).
- [96] J. Hooper, M. H. Fang, M. Zhou, D. Fobes, N. Dang, Z. Q. Mao, C. M. Feng, Z. A. Xu, M. H. Yu, C. J. O'Connor, G. J. Xu, N. Andersen, and M. Salamon, *Phys. Rev. B* **75**, 060403(R) (2007).
- [97] C. Piefke and F. Lechermann, *Physica Status Solidi B* **248**, 2269 (2011).
- [98] M. Behrmann, C. Piefke, and F. Lechermann, *Phys. Rev. B* **86**, 045130 (2012).
- [99] C. Autieri, M. Cuoco, and C. Noce, *Phys. Rev. B* **89**, 075102 (2014).
- [100] S. Mukherjee and W.-C. Lee, *Phys. Rev. B* **94**, 064407 (2016).
- [101] P. Rivero, V. Meunier, and W. Shelton, *Phys. Rev. B* **97**, 134116 (2018).
- [102] P. Rivero, R. Jin, C. Chen, V. Meunier, E. Plummer, and W. Shelton, *Sci. Rep.* **7**, 10265 (2017).
- [103] P. Steffens, J. Farrell, S. Price, A. P. Mackenzie, Y. Sidis, K. Schmalzl, and M. Braden, *Phys. Rev. B* **79**, 054422 (2009).
- [104] D. J. Singh and I. I. Mazin, *Phys. Rev. B* **63**, 165101 (2001).
- [105] I. Hase and Y. Nishihara, *J. Phys. Soc. Jpn.* **66**, 3517 (1997).
- [106] W. C. Lee, D. P. Arovas, and C. Wu, *Phys. Rev. B* **81**, 184403 (2010).
- [107] M. Cococcioni and S. de Gironcoli, *Phys. Rev. B* **71**, 035105 (2005).
- [108] M. A. Hossain, I. Zegkinoglou, Y.-D. Chuang, J. Geck, B. Bohnenbuck, A. G. C. Gonzalez, H.-H. Wu, C. Schüßler-Langeheine, D. G. Hawthorn, J. D. Denlinger, R. Mathieu, Y. Tokura, S. Satow, H. Takagi, Y. Yoshida, Z. Hussain, B. Keimer, G. A. Sawatzky, and A. Damascelli, *Sci. Rep.* **3**, 2299 (2013).
- [109] M. A. Hossain, Z. Hu, M. W. Haverkort, T. Burnus, C. F. Chang, S. Klein, J. D. Denlinger, H.-J. Lin, C. T. Chen, R. Mathieu, Y. Kaneko, Y. Tokura, S. Satow, Y. Yoshida, H. Takagi, A. Tanaka, I. S. Elfimov, G. A. Sawatzky, L. H. Tjeng, and A. Damascelli, *Phys. Rev. Lett.* **101**, 016404 (2008).
- [110] G. Li, Q. Li, M. Pan, B. Hu, C. Chen, J. Teng, Z. Diao, J. Zhang, R. Jin, and E. W. Plummer, *Sci. Rep.* **3**, 2882 (2013).
- [111] B. Hu, G. T. McCandless, V. O. Garlea, S. Stadler, Y. Xiong, J. Y. Chan, E. W. Plummer, and R. Jin, *Phys. Rev. B* **84**, 174411 (2011).
- [112] C. Autieri, *J. Phys.: Condens. Matter* **28**, 426004 (2016).
- [113] J. Leshen, M. Kawai, I. Giannakis, Y. Kaneko, Y. Tokura, S. Mukherjee, W.-C. Lee, and P. Aynajian, *Commun. Phys.* **2**, 36 (2019).
- [114] P. Rivero, V. Meunier, and W. Shelton, *Phys. Rev. B* **95**, 195106 (2017).
- [115] D. O. Brodsky, M. E. Barber, J. A. N. Bruin, R. A. Borzi, S. A. Grigera, R. S. Perry, A. P. Mackenzie, and C. W. Hicks, *Sci. Adv.* **3**, e1501804 (2017).

- [116] P. B. Marshall, K. Ahadi, H. Kim, and S. Stemmer, *Phys. Rev. B* **97**, 155160 (2018).
- [117] A. Subedi and D. J. Singh, *Phys. Rev. B* **81**, 024422 (2010).
- [118] D. J. Singh, *Phys. Rev. B* **67**, 054507 (2003).
- [119] D. J. Singh, *Phys. Rev. B* **92**, 174403 (2015).
- [120] W. Brzezicki, C. Noce, A. Romano, and M. Cuoco, *Phys. Rev. Lett.* **114**, 247002 (2015).